Dynamic Visualization of a Metal-Oxide-Surface/Gas-Phase Reaction: Time-Resolved Observation by Scanning Tunneling Microscopy at 800 K

Hiroshi Onishi and Yasuhiro Iwasawa
Department of Chemistry, Graduate School of Science, The University of Tokyo, Hongo, Bunkyo-ku, Tokyo 113, Japan

(Received 21 July 1995)

A surface/gas-phase reaction on $TiO_2(110)$ was visualized *in situ* by scanning tunneling microscopy. When a vacuum annealed (1×1) surface heated at 800 K was exposed to an O_2 ambient of 1×10^{-5} Pa, hill-like structures were randomly nucleated over terraces. Then they were transformed into new terraces, with added rows comprising double strands. We proposed a reoxidation scheme to interpret the dynamics; partially reduced Ti^{n+} ions ($n \leq 3$), which had been accumulated at interstitial positions in the vacuum annealed crystal, were oxidized at the surface to form the hills, added rows, and new terraces.

PACS numbers: 68.35.Dv, 68.35.Bs, 68.35.Fx, 68.35.Rh

The surface reaction of metal oxides especially under reactive atmospheres plays a crucial role in many technological processes, catalysis, corrosion, gas sensing, and oxide-film growth for dielectric or superconducting materials used in electronic devices. Dynamic observation during the surface reaction is indispensable for understanding how those processes occur on the oxide surfaces. This kind of information also helps us to consider the relation of surface structure to reactivity, a fundamental issue in surface physics and chemistry. For ionic compounds such as metal oxides, coordination around individual atoms perturbs their oxidation state, electronic configuration, and hence chemical reactivity in a much more prominent way than it does for metals or covalent semiconductors [1]. We report here the first atomic-scale dynamic visualization of a surface/gas-phase reaction of a metal oxide by scanning tunneling microscopy (STM).

Rutile TiO_2 is a typical transition-metal oxide widely used as a catalytic material and as a photoelectrode. It formally comprises Ti^{4+} and O^{2-} ions. Each Ti^{4+} ion is coordinated to an octahedron of six O^{2-} ions in the bulk [2], while oxygen octahedra left vacant form a channel along the [001] axis. Experimental studies have established that a $TiO_2(110)$ surface prepared by argon ion sputtering and vacuum annealing exhibits a (1×1)-ordered structure, for which a truncated stoichiometric model [Fig. 1(a)] is developed [1]. One-dimensional rows of Ti^{4+} ions and ridges of O^{2-} ions are assumed in the model. Recent STM studies [3–8] have found regular rows parallel to the [001] direction on (1×1) surfaces, and assigned them to the unoccupied states localized on the exposed Ti row. Those studies further found a protruding rowlike structure composed of double strands. Figure 1(b) presents constant current topography of a vacuum annealed (110) surface recorded at room temperature. Twelve double-strand rows are observed on (1×1) terraces. The exposed Ti rows regularly spaced 0.65 nm apart are resolved on the upper terrace. Hill-like features (sometimes the upper terrace) terminate the double-strand rows. The interpretation of the double-strand topography remains controversial; an added Ti_2O_3 row model [Fig. 1(a)] [4] and three types of missing-oxygen row models [3,6,9] have been proposed. A more recent STM study of a DCOO-covered $TiO_2(110)$ surface [8], where the position of the Ti ions was probed by imaging adsorbed $DCOO^-$ ions, revealed the absence of exposed Ti ions on the double-strand row. This gives strong evidence for the added Ti_2O_3 row model as a surface-limited phase of titanium oxide [8]. The added row model is thus employed to interpret the results in the present work. We assume that tunneling into vacant states of Ti^{3+} atoms in the added row causes the double-strand topography. The Ti^{3+} sites are 0.16 nm closer to the tip than the Ti^{4+} sites in plane.

The experiments were performed in a scanning tunneling microscope (JEOL-JSTM4500VT) with a base pressure of 2×10^{-8} Pa. Constant current topography was continuously determined (37 s/frame) and recorded on video. A Pt-Ir tip was used applying positive bias voltages on the sample. A polished $TiO_2(110)$ wafer of $6.5 \times 1 \times 0.25$ mm^2 (Earth Chemicals Co., Ltd., Japan) become deep blue and gave a (1×1) LEED pattern, after cycles of Ar^+ sputtering (3 keV, 0.3 μA) and vacuum annealing at 900 K [4,8]. An IR radiation thermometer monitored the temperature of the crystal. A small deficiency in oxygen concentration, 0.001%, was estimated from bulk resistivity of the blue crystal, 2 Ω m [10]. Research grade O_2 gas dried through a liquid N_2 trap was dosed in the chamber.

Constant current topography of the $TiO_2(110)$-(1×1) surface prepared by vacuum annealing at 900 K was determined maintaining the crystal at 800 K. Figure 2 presents some of the serial images of a square region (96×93 nm^2). In UHV [Figs. 2(a) and 2(b)], protruding rows (1.2 nm wide and 0.2 nm high) and small dots (1.2 nm diam and 0.3 nm high) were observed. The dimensions of the row and dot were compatible to those of the double-strand Ti_2O_3 row and hill-like structure [4,8]. Thus, the row and dot are assigned to Ti_2O_3 added row and isolated hill-like structure without a Ti_2O_3 row to be

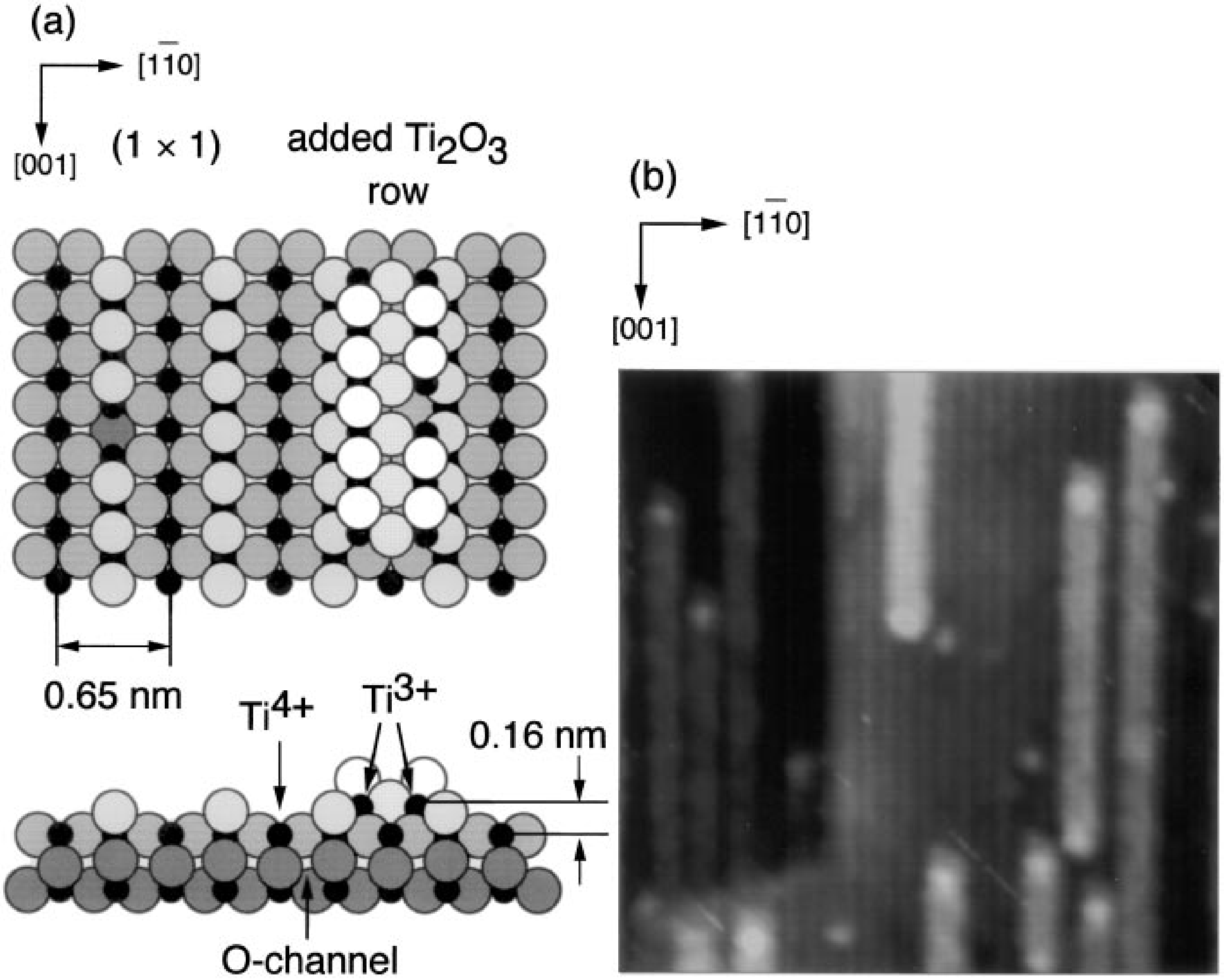

FIG. 1. TiO$_2$(110)-(1×1) surface with double-strand rows [4,8]. (a) Added Ti$_2$O$_3$ row model. Filled and shaded circles represent Ti and O ions, respectively. Plan and side views are shown. Point vacancies of the oxygen ion are created for illustration. (b) A constant current topography $(21 \times 21\ \text{nm}^2)$ of the (1×1) surface with double-strand rows, recorded at room temperature. Sample bias voltage: $+1.0$ V; tunneling current: 0.4 nA.

terminated, respectively. At this elevated temperature, the Ti$_2$O$_3$ rows fluctuated along their [001] axis, while the hills appeared and disappeared scan by scan.

When an O$_2$ ambient $(1 \times 10^{-5}\ \text{Pa})$ was dosed in the chamber, many hills were randomly nucleated over the terraces [Figs. 2(c)–2(e)]. The hills were then transformed to added Ti$_2$O$_3$ rows [Fig. 2(f)]. Spikes in the images reflect vigorous movements of surface atoms. Existing terraces became larger and new terraces appeared in Fig. 2(f). Nucleation and subsequent transformation were completed within 500 s in the ambient. An elongated feature of strong contrast in the upper right corner of Fig. 2(f) is likely multistacked terraces. The added rows and small terraces in Fig. 2(f) gradually depopulated with time. Figure 2(g) presents topography of the surface exposed to the ambient for 780 s. (The imaged field was shifted to the left by 40 nm to avoid the multistacked region.) Added rows and new terraces shrank in average during O$_2$ exposure between Figs. 2(f) and 2(g). The oxygen dose was then closed maintaining the crystal at 800 K. Figure 2(h) was recorded on the surface left in vacuum $(2 \times 10^{-8}\ \text{Pa})$ for 1200 s. No abrupt response to the evacuation was observed. Added rows and small terraces continued to diminish.

Figure 3 shows a set of small area $(31 \times 30\ \text{nm}^2)$ scans including two new terraces observed in the left side of Fig. 2(f). Added Ti$_2$O$_3$ rows and new terraces dynamically fluctuated. The regular lines of the Ti row spaced 0.65 nm apart were resolved on the existing and new terraces, indicating that they maintained the (1×1) structure even in the oxygen ambient at 800 K.

The formation of the additional structures [i.e., hill, added Ti$_2$O$_3$ row, and (1×1) terrace] is apparently caused by reaction of the substrate with the O$_2$ ambient. A H$_2$ ambient of 1×10^{-5} Pa instead of oxygen did not affect a (110) surface heated at 800 K at all. A tip-induced

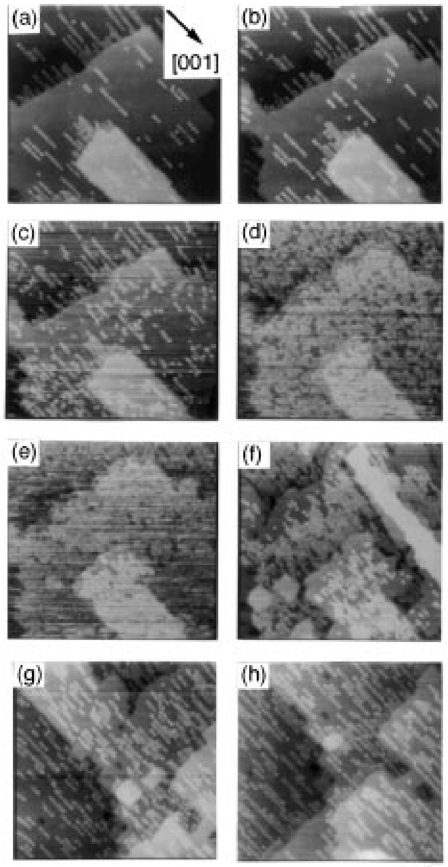

FIG. 2. Serial constant current images (96×93 nm^2) of a $TiO_2(110)$-(1×1) surface maintained at 800 K. Images (a)–(h) were successively determined at $t = 0$, 220, 550, 630, 670, 740, 1520, and 3800 s, respectively. Images (a) and (b) were observed in UHV before O_2 dose. An O_2 atmosphere of 1×10^{-5} Pa was dosed at $t = 260$ s and evacuated at $t = 2600$ s. Sample bias voltage: +1.5 V; tunneling current: 0.3 nA.

effect was also excluded. A postexposure imaging found similar Ti_2O_3 row formation on an oxygen-exposed $TiO_2(110)$ surface, where the tip was retracted away from the surface during oxygen dose at 800 K. Cross-linking structures reported on a $TiO_2(110)$ surface annealed in O_2 at 1000 K [3,7] were not observed in our experiments.

We believe that partially reduced Ti^{n+} ($n \leq 3$) ions nonstoichiometrically present in the substrate were reoxidized by the O_2 ambient into additional structures. This process continued until the Ti^{n+} ions accessible to the surface were exhausted. The finite deficiency in oxygen concentration (0.001%) leads to a complementary amount of Ti^{n+} ions in the vacuum annealed crystal. It is well known that Ar^+ bombardment and vacuum annealing result in Ti-rich (O-deficient) compositions on titanium oxide surfaces [1]. The excess Ti^{n+} ions had probably been accumulated in oxygen octahedra which should be vacant in a genuine TiO_2 crystal. Indeed, trivalent and tetravalent Ti ions have been proposed to occupy interstitial positions in TiO_{2-x} crystals reduced in a CO-CO_2 mixture at 1200–1700 K [11]. Displacement of low valence Ti ions to interstitial sites is also assumed to initiate the formation of crystallographic shear structures (Ti_nO_{2n-1}), Magnéli phases [12]. On the other hand, the reduced composition of a sputter-annealed surface has often been related to oxygen vacancies assuming metal ions of reduced coordination left their original position [1]. However, such O vacancies would be simply refilled in the O_2 ambient and could not be responsible for the formation of additional structures. This argument supports the interpretation of the double-strand row structure as a Ti_2O_3 added row. The missing oxygen row models [3,6,9] cannot explain that an oxygen ambient promotes row creation on a stoichiometric (1×1) surface.

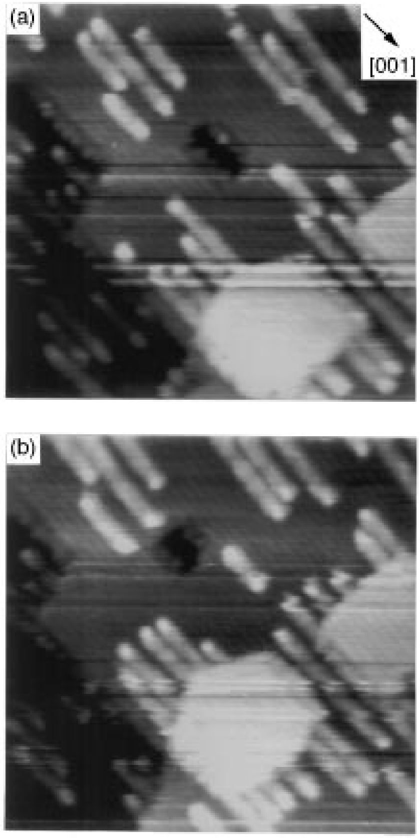

FIG. 3. Small area (31×30 nm^2) scans of the $TiO_2(110)$ surface in Fig. 2. Images (a) and (b) were observed at $t =$ 2220 and 2370 s, respectively, in the O_2 ambient at 800 K. Sample bias voltage: +1.5 V; tunneling current: 0.3 nA.

Employing this reoxidation scheme, the random nucleation of hills [Figs. 2(c)–2(e)] suggests that Ti^{n+} ions to be oxidized migrated vertically from the bulk to the surface, by hopping from one O octahedron to another. The fluctuation of hills and Ti_2O_3 rows observed in UHV and in the O_2 ambient indicates that mass transport is thermally activated at 800 K independent of ambient. It seems that Ti^{n+} ions are not detached from step sites to diffuse over the terrace. The detachment and in-plane diffusion might result in nucleation localized in the vicinity of steps. This was not the case. Detached Ti ions should be highly unstable due to reduced coordination. The vertical transport of Ti ions contrasts with the surface migration of neutral Cu atoms on the Cu(110) surface, where mobile metal atoms migrate over the terrace even at room temperature [13].

On the other hand, the axial fluctuation of the Ti_2O_3 row (Fig. 3) suggests mass transport along the row axis. The added row model [Fig. 1(a)] comprises double channels of oxygen octahedra occupied by Ti^{3+} ions. We assume that Ti transfer through the channels causes axial fluctuation of the added row. The O-octahedra channel in bulk TiO_2 [Fig. 1(a)] provides an anisotropic way for metal atom diffusion [14].

Finally, stability of the surface oxides is considered. The low valent Ti ions are oxidized by the O_2 ambient as follows: interstitial ions in bulk TiO_2 → hill-like TiO_x → added Ti_2O_3 row → $TiO_2(110)$-(1×1) terrace. The reverse reaction did not take place even in vacuum, probably because of being kinetically hindered. It seems unusual that an oxidative atmosphere promoted the formation of reduced oxides on a TiO_2 substrate. This apparent contradiction is resolved by considering the kinetically controlled transitions among the metastable phases. Hill-like TiO_x, the first product in the reaction, were irreversibly transformed to Ti_2O_3 rows. This suggests that the hill-like oxide is kinetically more favorable but thermodynamically less stable than the row is. In fact, hills could not be transformed further at 600 K even under the O_2 atmosphere. Added Ti_2O_3 rows once formed gradually depopulated on a larger time scale. This indicates that the row is also a metastable phase to be slowly converted to the $TiO_2(110)$-(1×1) terrace, the most stable phase in the ambient. Small terraces are diminished to reduce energetically unfavorable step sites.

In summary, a surface/gas-phase reaction on a vacuum annealed $TiO_2(110)$-(1×1) surface has been visualized by dynamic STM. Hill-like oxide, added Ti_2O_3 row, and a new (1×1) terrace were formed in the oxygen ambient. We propose a reoxidation scheme to interpret the dynamics; partially reduced Ti^{n+} ions $(n \leq 3)$, which had been accumulated at interstitial positions in the crystal, were transported and oxidized at the surface. Axial fluctuation of the Ti_2O_3 row suggests Ti transport through the double channels of oxygen octahedra in the row. The present study demonstrates that interstitial Ti ions are mobile and reactive to an oxidative atmosphere. Such metal interstitials and resultant surface oxides may have considerable importance in many technological processes on metal oxides, while nonstoichiometric structures at oxide surface have often been associated with O-vacancy creation [1].

[1] V. E. Henrich and P. A. Cox, *The Surface Science of Metal Oxides* (Cambridge University Press, Cambridge, 1994).

[2] R. W. G. Wykcoff, *Crystal Structure* (Wiley, New York, 1965), 2nd ed., Vol. 1, p. 251.

[3] M. Sander and T. Engel, Surf. Sci. Lett. **302**, L263 (1994).

[4] H. Onishi and Y. Iwasawa, Surf. Sci. Lett. **313**, L783 (1994).

[5] D. Novak, E. Garfunkel, and T. Gustafsson, Phys. Rev. B **50**, 5000 (1994).

[6] P. W. Murrey, N. G. Condon, and G. Thornton, Phys. Rev. B **51**, 10 989 (1995).

[7] A. Szabo and T. Engel, Surf. Sci. **329**, 241 (1995).

[8] H. Onishi, K. Fukui, and Y. Iwasawa, Bull. Chem. Soc. Jpn. **68**, 2447 (1995).

[9] P. J. Møller and M.-C. Wu, Surf. Sci. **224**, 265 (1989).

[10] H. Onishi and Y. Iwasawa, Jpn. J. Appl. Phys. **33**, L1338 (1994).

[11] P. Kofstad, J. Less-Common Metals **13**, 635 (1967).

[12] S. Andersson and A. D. Wadsley, Nature **211**, 581 (1966).

[13] J. Wintterlin, R. Schuster, D. J. Coulman, G. Ertl, and R. J. Behm, J. Vac. Sci. Technol. B **9**, 902 (1991).

[14] J. L. Steele and E. R. McCartney, Nature **222**, 79 (1969).